The Antarctic Demonstrator for the Advanced Particle-astrophysics Telescope (ADAPT)

Di Venere L.[1], De Palma G.[1,2], Licciulli F.[1], for the APT collaboration

[1]Istituto Nazionale di Fisica Nucleare, Sezione di Bari, I-70126 Bari, Italy
[2]Politecnico di Bari, Department of Mechanics, Mathematics and Management, via Orabona, 4, I-70125 Bari, Italy

E-mail: leonardo.divenere@ba.infn.it

Abstract. The Antarctic Demonstrator for the Advanced Particle-astrophysics Telescope (ADAPT) is a suborbital mission designed to detect MeV to GeV gamma rays. The instrument consists of four layers of a scintillating fiber tracker plus an active converter tracker made of CsI scintillating crystals read out by wavelength shifting (WLS) fibers. Both scintillating and WLS fiber signals will be detected with Silicon Photomultipliers (SiPM). Fast and low power front-end electronics are being developed based on the SMART ASIC for SiPM signal amplification before the successive digitization stage. The ADAPT project will serve as technology demonstrator for the larger Advanced Particle-astrophysics Telescope (APT) mission, which will have a much larger area of 3×3 m^2. The ADAPT instrument will feature a 30-day balloon flight, with the possibility of detecting prompt signals from Gamma-Ray Bursts (GRBs) with degree-scale localization and polarization constraints. In this contribution, we will present the ADAPT project and its current status, with a particular focus on the frontend electronics development.

1 Introduction

In recent years, gamma-ray astronomy has proved to be a powerful energy domain to investigate the most energetic events in the Universe. Successful space experiments, such as the AGILE and Fermi missions allowed the Universe observation at energies above 100 MeV, leading to important discoveries. However, current missions have poor sensitivities in the so called "medium-energy" gamma-ray range, namely between tens of keV to few hundreds of MeV. Several missions have been proposed for the next generation of gamma-ray satellite experiments to cover this energy range[1, 2]. The Advanced Particle-astrophysics Telescope (APT) is a proposed space-based experiment designed to detect MeV to TeV gamma rays and cosmic rays. APT will also feature a wide field of view, enhancing the capability of detecting and localizing low energy transient gamma-ray sources. This feature will be also ideal in the era of multi-wavelength and multi-messenger astrophysics [3].

2 The Advanced Particle-astrophysics Telescope concept

APT design will combine a pair tracker and Compton telescope in a single design. It will include multiple layers of scintillating fiber tracker hodoscopes readout by Silicon Photomultipliers (SiPMs) and a distributed Imaging CsI Calorimeter (ICC), consisting of CsI:Na scintillator tiles coupled to crossed planes of wavelength-shifting (WLS) fibers readout by SiPMs. The ICC design allows the localization of the energy deposition in the scintillator with ∼mm accuracy. An additional SiPM-based edge detector placed on the side of the CsI:Na tiles will enhance the scintillation light collection and improve the energy measurement. For both the Hodoscope and ICC, signals of few photoelectrons per channel are expected, requiring a high resolution readout to maximize the instrument performance.

This design will allow APT to work as both pair-conversion and Compton telescope, as illustrated in Fig.1. Gamma rays with energies above tens of MeV will undergo pair production, generating an electron-positron pair to be tracked by the scintillating fiber tracker layers. On the other side, low-energy gamma rays, namely with energy below few MeV, will interact mainly with the ICC via Compton scattering. The recoil electron will be absorbed in the ICC layer where the interaction occurred, while the scattered photon will be absorbed by a subsequent ICC layer. The WLS readout and the edge-detector will allow the precise localization of the two interactions and the measurement of the released energy, allowing the reconstruction of the Compton scattering angle.

The APT instrument will feature up to 20 interleaved ICC and fiber tracker layers, reaching a 3 m × 3 m × 2.5 m detector, which will improve the effective area by one order of magnitude compared to the current satellite experiments in the GeV range.

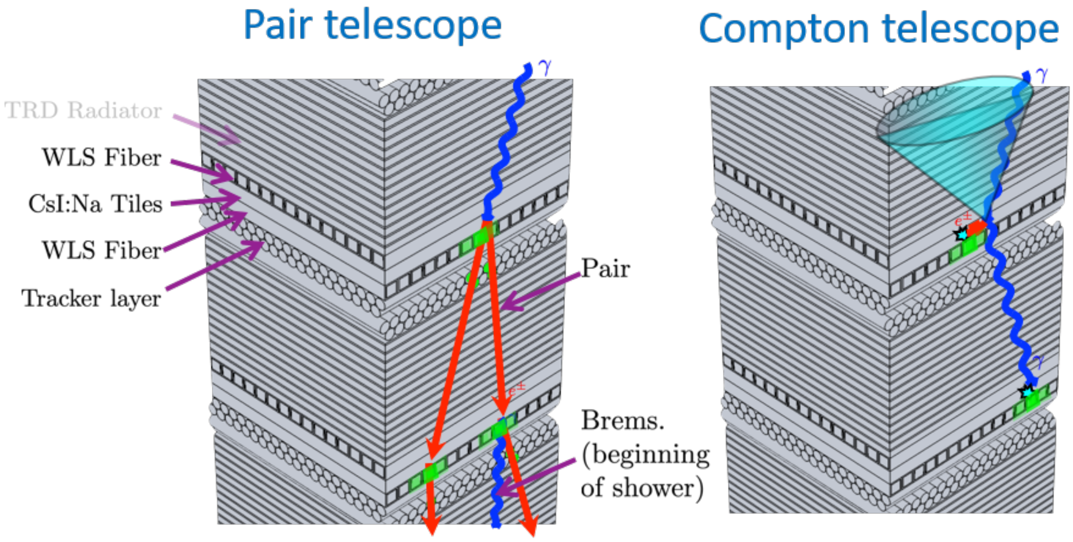

Figure 1: APT concept design. Left: schematic of the pair detection mechanism. Right: schematic of the Compton detection mechanism.

3 The Antarctic Demonstrator for APT (ADAPT)

The Antarctic Demonstrator for APT (ADAPT) is a prototype high-altitude balloon mission, anticipated to fly in Antarctica in the 2026-27 season. It features only 1% of the total amount of material that will be used for APT and will serve as a proof of concept for the APT concept. It will also provide reconstruction and localization of transient gamma-ray events and will provide real-time positional alerts for Gamma-Ray Bursts.

As shown in Fig.2, the ADAPT detector[3] stackup will consist of:

- *SSDs*: Silicon Strip Detectors (SSDs) for CR charge identification located on top of the detector;
- *ICCs*: Imaging CsI Calorimeter modules; 4 layers, each one consisting of 3×3 tiles of 15 cm × 15 cm × 15 mm of CsI(Na) crystals, with crossed 2×2 mm^2 WLS fibers with a SiPM readout to measure the position of the interaction and SiPM-based CsI edge detectors to measure the energy release;
- *Hodoscope*: 4 layers of X-Y crossed scintillating fiber tracker modules, with interleaved 1.5 mm scintillating fibers and a SiPM readout;
- *Tail Counters*: 4 layers of CsI modules equipped with only edge detector readouts for energy measurements.

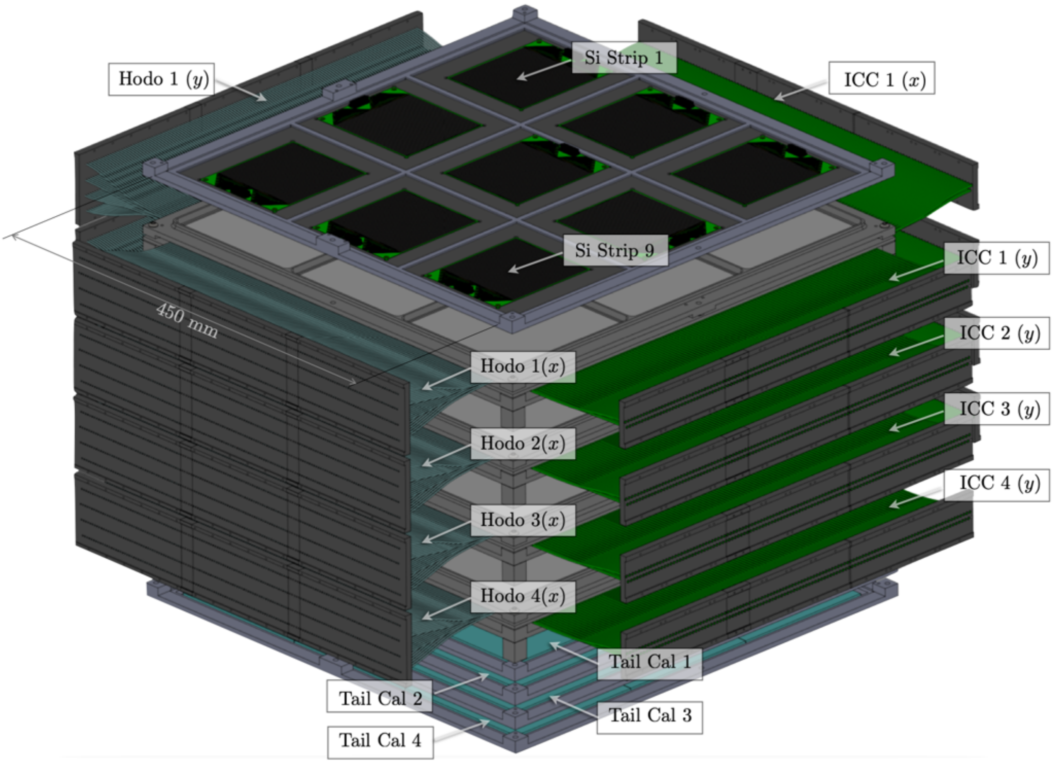

Figure 2: Stackup of the ADAPT balloon detector.

Several studies have been conducted to estimate the ADAPT detector performance through simulations [4, 5] and its capabilities to detect transient events such as Gamma-ray Bursts through real time reconstruction and localization algorithms [6]. In this contribution, we will focus on the electronics design and first tests of the Hodoscope and ICC subdetectors, together with a preliminary characterization of their performance.

4 Hodoscope and ICC readout design for ADAPT

As described in previous section, the hodoscope and ICC in ADAPT will feature four interleaved layers. Each layer will have a bundle of fibers (scintillating fibers and WLS fibers respectively) be stretched into a linear array. A custom board will host a SiPM array to have a one-to-one match between fibers and SiPMs. The following devices will be employed:

- Hamamatsu 3×3 mm^2 (S13360-3050CS) to match the 2×2 mm^2 WLS fibers;
- Hamamatsu 2×2 mm^2 (S13360-2050VE) to match the 1.5 mm round scintillating fibers of the Hodoscope.

An analog sum of three non-adjacent SiPMs is implemented, in order to reduce the number of electronics channels by a factor of 3 and limit the total power consumption of the instrument. In particular, the signals coming from corresponding SiPMs of each 15×15 cm^2 block of the instrument are summed together. This scheme does not degrade the performance of the detector in terms of localization capabilities, since the spatial pitch of adjacent readout channels is not changed. However, it introduces a degeneracy in the position reconstruction, since the interaction may come from any of the nine 15×15 cm^2 quadrants of the detector. To resolve this degeneracy, the edge detector is placed at one side of each ICC layer. This detector consists of a linear array of 3×3 mm^2 Hamamatsu SiPMs placed directly on the edge of the scintillator. The SiPM signals of each 15×15 cm^2 tile are summed together to provide the overall response of the scintillating tile. The signal provided by the edge detector will then uniquely identify the quadrant of the interaction, solving the degeneracy introduced by the multiplexer board. A more detailed description of this concept is provided in [7].

The readout electronics of the Hodoscope and ICC is based on a pre-amplification stage of the SiPM signals, followed by the digitization of the amplified pulses. The pre-amplification stage is based on the SMART, a 16-channel ASIC developed for the Cherenkov Telescope Array Observatory [8]. The SMART features a fast path with a tail suppression stage, with tunable gain, pulse shape and and pole-zero compensation. In addition, the SMART allows for the SiPM bias fine tuning on individual channels through internal DACs, in order to compensate for SiPM-to-SiPM gain variations. Two dedicated boards based on the SMART ASIC have been developed and tested, one for the Hodoscope and one for the ICC readout.

4.1 Hodoscope SMART electronics

The SMART Hodoscope board hosts three SMART ASICs, for a total of 48 readout channels. A total of 32 boards will be necessary to readout the full ADAPT instrument. A prototype phase was conducted to validate the performance of the SMART pre-amplification stage. A single 2×2 mm^2 Hamamatsu SiPM operated at 57 V was coupled to the SMART ASIC and illuminated with a pulsed LED. The output pulses were acquired through a Lecroy HDO6104B oscilloscope. Fig. 3 shows the amplitude distribution (left) and the single photoelectron (p.e.) pulse measured (right). The measured gain is 19.45±0.05 mV/p.e., with a signal-to-noise ratio of about 9. From the single p.e. waveform, the Full Width at Half Maximum (FWHM) and the recovery time were extracted with a gaussian and an exponential fit respectively. Several SMART configuration were tested, showing a gain tunable in the range [535]mV/p.e. and a FWHM of the pulse in the range [5-25] ns.

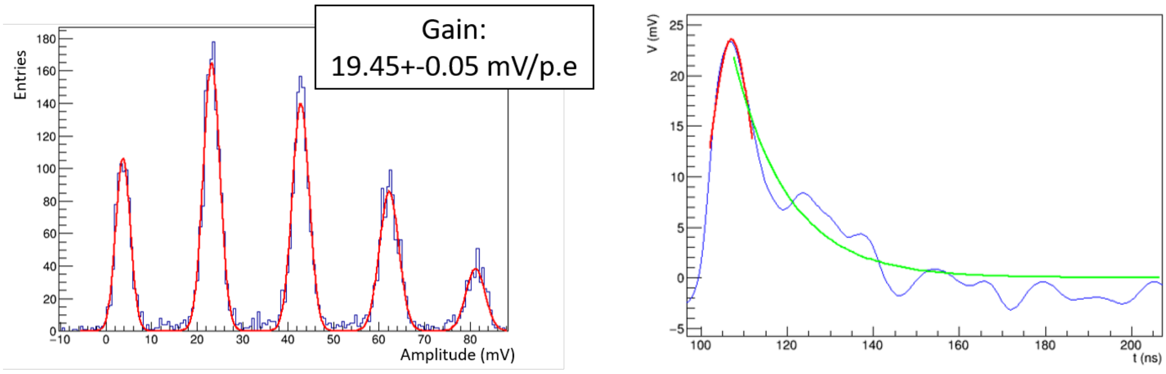

Figure 3: Left: amplitude distribution obtained from SMART output signals coupled to a 2×2 mm^2 S13360-2050VE Hamamatsu SiPM operated at 57 V. Right: single photoelectron pulse measured in the same conditions.

After the prototyping phase, a total of 40 Hodoscope SMART boards were produced and tested for the full ADAPT instrument. Quality control tests were performed coupling the SMART inputs to an array of 2×2 mm^2 Hamamatsu SiPMs (S13360-2050VE), operated at 57 V and illuminated with a pulsed LED. Three different SMART configurations and bias DAC were tested. For each channel, the mean waveforms were calculated and the FWHM and recovery time were extracted again through a gaussian and exponential fit. Plots in Fig.4 show the distributions of the measured FWHM and recovery time for all channels, confirming the expected behavior of the ASICs for all the boards tested.

4.2 ICC SMART electronics

A second electronics board based on the SMART ASIC was designed and produced for the readout of the ICC SiPMs. This board hosts five SMART ASICs for a total of 80 readout channels. Each board can be used to read out a single view of each layer of ADAPT. Hence, a total of 8 boards are necessary to equip the full ADAPT instrument (X and Y views for 4 layers).

A fast trigger circuit was also added in this board, which is based on a summer amplifier to sum and shape the 16 signals produced by each SMART ASIC. The summed signals are then sent to a discriminator with a tunable threshold. The logic OR of the five discriminated signals is finally used to generate a FAST trigger signal.

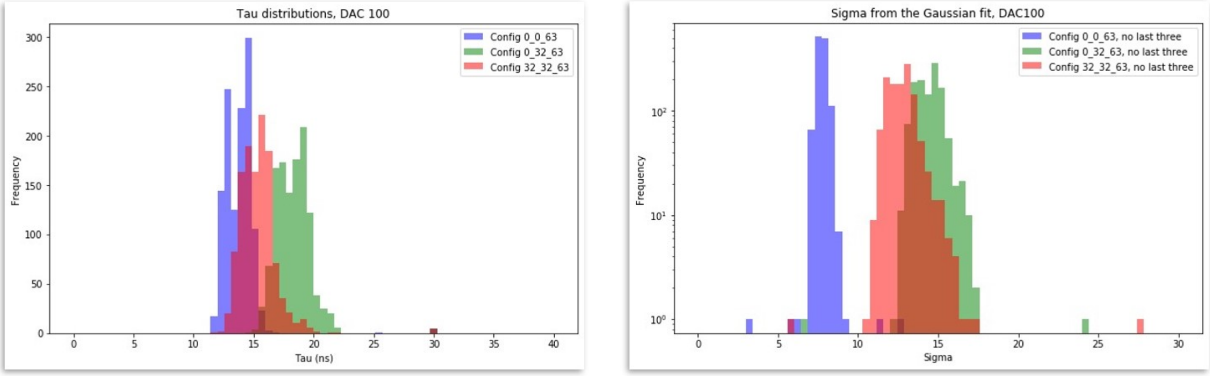

Figure 4: Quality control results on the SMART Hodoscope boards. Left: recovery time obtained from the exponential fit for the three different SMART configurations tested. Right: sigma from the gaussian fit for the same SMART configurations.

A first prototype board was produced and tested. An array of 3×3 mm^2 Hamamatsu SiPMs (S13360-3050CS) operated at 43 V was coupled to the SMART ICC board and illuminated with a pulsed LED. Fig. 5 shows the waveforms acquired from one SMART channel and the corresponding charge distribution as measured by a 16-channel digitizer board based on the CTC ASIC [9], developed for the Cherenkov Telescope Array Observatory.

The summer amplifier was also tested by acquiring the output of the summer amplifier through an oscilloscope. A single channel was fed into the board and the SMART and the summer amplifier outputs were acquired at the same time. The high resolution of the SMART signals allowed for a selection of the events of individual p.e., which were compared with the ones coming from the summer amplifier. Fig. 6 shows the amplitude distribution derived from the summer amplifier output. The overlaid distributions are obtained taking into account only the 1 p.e., 2 p.e. and 3 p.e. events selected from the SMART output.

The performance of the tested board were in agreement with the design specifications and the production for the full ADAPT instrument was started. The quality control tests on these boards are currently ongoing. Integration in the full ICC instrument is expected in mid 2025.

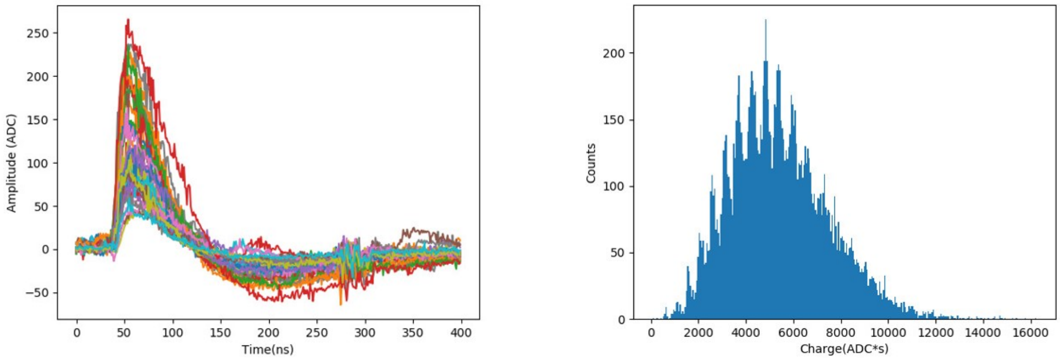

Figure 5: Left: waveforms acquired from one SMART channel of the ICC frontend board coupled to a 3×3 mm^2 Hamamatsu SiPMs (S13360-3050CS) as measured by a 16-channel digitizer board based on the CTC ASIC. Right: the corresponding charge distribution.

5 Conclusions

The ADAPT project is a demonstrator instrument for the future APT mission, which is aimed to fly on a 60 million-cubic-foot balloon flight from Antarctica. In this paper, we have presented the developments

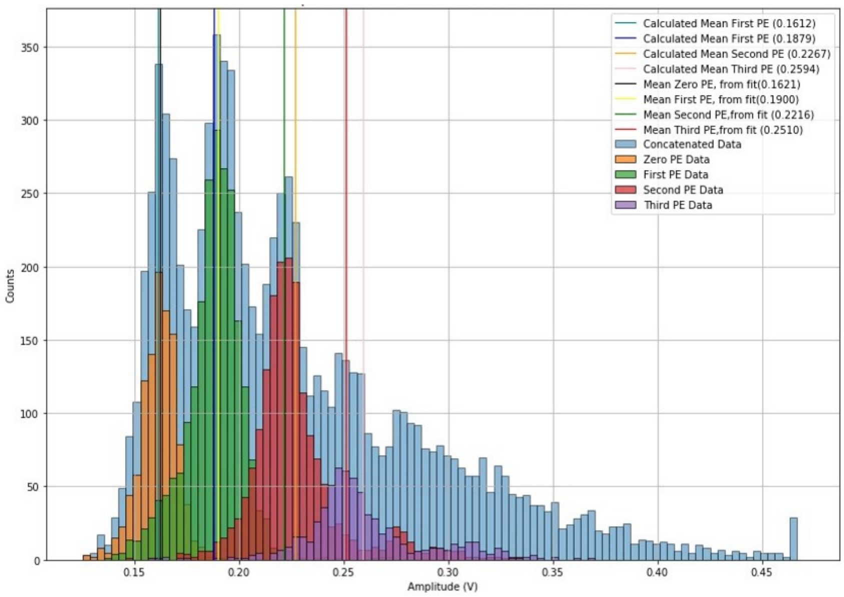

Figure 6: Amplitude distribution derived from the summer amplifier output. The orange, green, red and purple distributions are identify the 0 p.e., 1 p.e., 2 p.e. and 3 p.e. events selected from the SMART output. The vertical lines show the mean values mean of individual p.e. distributions, both as calculated from the histograms and from a gaussian fit.

and tests for the readout electronics of two sub-detectors of the ADAPT instrument, the Hodoscope and the ICC. The core of the design is based on the SMART, a 16-channel ASIC devoted to the pre-amplification of SiPM signals. The developed boards proved to reach single p.e. resolution for the detection of the low intensity signals produced in both the scintillating fibers of the Hodoscope and the WLS fibers of the ICC. All boards for the full ADAPT instruments were produced and partially tested. Integration of the electronics in the full ADAPT instrument is expected in mid 2025.

Acknowledgments

This work was supported by NASA award 80NSSC21K1741, NSF award CNS-1763503 and by Istituto Nazionale di Fisica Nucleare (INFN).

References

[1] De Angelis A., et al, ”Science with e-ASTROGAM: A space mission for MeV–GeV gamma-ray astrophysics”, Journal of High Energy Astrophysics 19 (2018) 1-106

[2] McEnery J., et al., ”All-sky Medium Energy Gamma-ray Observatory: Exploring the Extreme Multimessenger Universe”, arXiv:1907.07558

[3] Buckley J. et al., ”The Advanced Particle-astrophysics Telescope (APT) Project Status”, in Proc. of 37th Int’l Cosmic Ray Conference, vol. 395, pp. 655:1–655:9, July, 2021, https://doi.org/10.22323/1.395.0655.

[4] Chen W. et al., ”The Advanced Particle-astrophysics Telescope: Simulation of the Instrument Performance for Gamma-Ray Detection”, in Proc. of 37th Int’l Cosmic Ray Conference, vol. 395, 590, 2021, https://doi.org/10.22323/1.395.0590.

[5] Chen W. et al., ”Simulation of the instrument performance of the Antarctic Demonstrator for the Advanced Particle-astrophysics Telescope in the presence of the MeV background” in Proc. of 38th Int’l Cosmic Ray Conference, vol. 444, 841, 2023, https://doi.org/10.22323/1.444.0841

[6] Sudvarg M. et al., ”A Fast GRB Source Localization Pipeline for the Advanced Particle-astrophysics Telescope”, in Proc. of 37th Int’l Cosmic Ray Conference, vol. 395, 588, July, 2021, https://doi.org/10.22323/1.395.0588.

[7] Sudvarg M. et al., "Front-End Computational Modeling and Design for the Antarctic Demonstrator for the Advanced Particle-astrophysics Telescope" in Proc. of 38th Int'l Cosmic Ray Conference, vol. 444, 764, 2023, https://doi.org/10.22323/1.444.0764

[8] C.Aramo et al., "A SiPM multichannel ASIC for high Resolution Cherenkov Telescopes (SMART) developed for the pSCT camera telescope", Nuclear Instruments and Methods in Physics Research Section A: Accelerators, Spectrometers, Detectors and Associated Equipment, 1047 (2023) 167839, https://doi.org/10.1016/j.nima.2022.167839

[9] Schwab B. et al, "CTC and CT5TEA: An advanced multi-channel digitizer and trigger ASIC for imaging atmospheric Cherenkov telescopes", Nuclear Instruments and Methods in Physics Research Section A: Accelerators, Spectrometers, Detectors and Associated Equipment, 1069 (2024) 169841, https://doi.org/10.1016/j.nima.2024.169841